Changes in crystalline lens radii of curvature and lens tilt and decentration during dynamic accommodation in Rhesus Monkey

6

6. Changes in crystalline lens radii of curvature and lens tilt and decentration during dynamic accommodation in Rhesus Monkey

This chapter is based on the article by de P. Rosales et al., *"Changes in crystalline lens radii of curvature and lens tilt and decentration during dynamic accommodation in Rhesus Monkey"* (Journal of Vision In press). Coauthors of the study are M. Wendt, S. Marcos, A. Glasser. The contribution of Patricia Rosales to the study was to prepare the processing algorithm for dynamic measurement of phakometry, and to measure lens tilt and decentration for each accommodative state in Rhesus Monkeys. Part of the study was conducted in the University of Houston College of Optometry (Adrian Glasser's lab).

RESUMEN

Objetivos: Estudiar cómo cambian los radios de curvatura del cristalino del Rhesus Monkey en función de la acomodación dinámica y medir los cambios en la inclinación y descentramiento del cristalino para cada estado acomodativo.

Métodos: Las medidas de los cambios en los radios de curvatura del cristalino y de la inclinación y descentramiento durante la acomodación dinámica centralmente estimulada, se realizaron en cuatro ojos de dos monos adolescentes. Las medidas dinámicas de facometría se realizaron mediante un video facómetro basado en imágenes de Purkinje. Los radios de curvatura de las caras anterior y posterior del cristalino se calcularon a partir de reflexiones de dobles LEDs procedentes de las diferentes superficies oculares (Imágenes de Purkinje PI, PIII y PIV). La inclinación y descentramiento del cristalino se calcularon asumiendo una relación lineal entre las posiciones de las imágenes de Purkinje, rotación del ojo, inclinación y descentramiento del cristalino. Como los ojos del mono estaban iridectomizados, se tomó como referencia para las posiciones de las imágenes de Purkinje el punto medio de la primera doble imagen de Purkinje (PI).

Resultados: El valor medio obtenido de los radios de curvatura de las caras anterior y posterior del cristalino en estado desacomodado fue 11.11±1.58 mm y -6.64±0.62 mm, respectivamente. Se encontró una disminución de los radios de curvatura aproximadamente lineal con la acomodación para todos los ojos, a razón de 0.48±0.14 mm/D y 0.17 ± 0.03 mm/D para las superficies anterior y posterior del cristalino, respectivamente. Para la inclinación y el descentramiento no se encontraron cambios significativos con la acomodación, excepto para la inclinación vertical (0.147± 0.25 deg/D).

Conclusiones: Se ha desarrollado un sistema de medida y procesado de los cambios de los radios de curvatura, inclinación y descentramiento

del cristalino durante la acomodación dinámica, encontrándose un cambio lineal de los radios de curvatura del cristalino durante la acomodación, mientras que la inclinación y descentramiento del cristalino apenas cambian durante la acomodación, excepto para la inclinación vertical. Estos resultados son importantes para una completa caracterización del proceso acomodativo en el Rhesus Monkey.

ABSTRACT

Purpose: To measure dynamic changes in crystalline lens radii of curvature and lens tilt and decentration during centrally stimulated accommodation in four iridectomized eyes of two adolescent rhesus monkeys.

Methods: Phakometry measurements were performed dynamically using a custom-built, video-based, Purkinje-image instrument. Lens anterior and posterior radii were calculated from reflections of paired light sources from the ocular surfaces (Purkinje images PI, PIII and PIV). Lens tilt and decentration were calculated assuming linearity between Purkinje image positions, eye rotation, lens tilt and decentration. Because the monkey eyes were iridectomized, Purkinje images were referred to the mid-point of the double first Purkinje image (PI).

Results: Mean unaccommodated values of anterior and posterior lens radii of curvature were 11.11±1.58 mm and -6.64±0.62 mm respectively, and these decreased relatively linearly with accommodation in all eyes, at a rate of 0.48±0.14 mm/D and 0.17 ± 0.03 mm/D for anterior and posterior lens surfaces respectively. Tilt and decentration did not change significantly with accommodation except for tilt around the horizontal axis which changed at a rate of 0.147± 0.25 deg/D.

Conclusions: A system and a method to measure and to process dynamic changes in lens radii of curvature and lens tilt and decentration during centrally stimulated accommodation has been presented, finding a linear change of lens radii during accommodation, while lens tilt and decentration did not change significantly during accommodation, except for vertical tilt. Those results are important to fully characterize the accommodative process in the rhesus monkey.

1. INTRODUCTION

Accommodation is an increase in the dioptric power of the eye that enables the image of near objects to be focused on the retina. As described in the Introduction, according to the classic Helmholtz mechanism of accommodation (Von Helmholtz, 1855), during distant vision (when the lens is unaccommodated), the ciliary muscle is relaxed, the zonular fibers are under tension and the lens is pulled flat. During accommodation, the ciliary muscle contracts, releasing tension on the zonular fibers at the lens equator, allowing the lens equatorial diameter to decrease, the lens thickness to increase, and the lens anterior surface to become more steeply curved.

While axial changes in lens position, and centripetal movements of the crystalline lens have been studied in detail, to our knowledge only one human study has looked at possible changes in crystalline lens tilt and decentration (in the horizontal direction) for unaccommodated and accommodated eyes (Kirschkamp, Dunne & Barry, 2004), for an accommodative demand of 4 D. The change in crystalline lens shape and alignment has implications for the accommodative mechanism and for accommodative optical performance. Optical aberrations have been measured for different accommodative demands in humans, both statically (Cheng, Barnett, Vilupuru, Marsack, Kasthurirangan, Applegate & Roorda, 2004, He, Burns & Marcos, 2000) or dynamically (Hofer, Artal, Singer, Aragon & Williams, 2001) as well as in enucleated monkey eyes (Roorda & Glasser, 2004) and dynamically in iridectomized centrally stimulated monkeys (Vilupuru, Roorda & Glasser, 2004). These studies all report a consistent shift of spherical aberration with accommodation toward more negative values (which must be related to changes in the lens shape and/or gradient index distribution). An increase in vertical coma with accommodation is shown in some humans (Cheng et al., 2004, Plainis, Ginis & Pallikaris, 2005) and monkeys (Vilupuru et al., 2004), suggesting an increase in the lens vertical decentration and/or tilt. Other studies have examined the potential role of monochromatic aberrations on accommodation dynamics (Chen, Kruger, Hofer, Singer & Williams, 2006, Fernandez & Artal, 2005, Radhakrishnan & Charman, 2007).

In the study presented in this Chapter, ocular biometry and infrared photorefraction were measured dynamically during Edinger-Westphal (EW) stimulated accommodation in anesthetized, iridectomized rhesus monkeys for identical stimulus current amplitudes. Changes in anterior and posterior crystalline lens radii, lens tilt and decentration were

also measured dynamically for the same stimulus amplitudes using a custom-built phakometry Purkinje imaging technique. Those measurements, together with biometric and photorefractive measurements in monkey eyes (Vilupuru & Glasser, 2005), are useful to fully characterize the accommodative mechanism in a widely accepted animal model for human accommodation and presbyopia (Glasser & Kaufman, 1999, Glasser, Wendt & Ostrin, 2006, Koretz, Bertasso, Neider, True-Galbelt & Kaufman, 1987a).

2. METHODS

2.1 Animals

The left and right eyes of two anesthetized rhesus monkeys (#54 and #58) were imaged during EW stimulated accommodation. The monkeys were aged 9 years, 1 month and 9 years, 3 months respectively and had previously undergone complete, bilateral removal of the irides (Kaufman & Lütjen-Drecoll, 1975) and surgical implantation of stimulating electrodes into the EW nucleus (Chen & Makous, 1989). All experiments followed the ARVO Statement for the Use of Animals in Ophthalmic and Vision Research and were performed in accordance with institutionally approved animal protocols.

2.2 Measurement of current stimulus /accommodative response

At the start of each experiment, a Hartinger coincidence refractometer (Zeiss, Jena, Germany) was used to measure the static accommodative response for each eye as a function of increasing stimulus amplitudes. Baseline refraction and maximal accommodated refraction achieved at each stimulus amplitude was recorded. Accommodative amplitude at each stimulus current amplitude was the difference between these two refractions.

2.3 Dynamic measurement of accommodation

Infrared photorefraction was used to measure dynamic changes in refractive state during centrally stimulated accommodation (Glasser & Kaufman, 1999, Schaeffel, Farkas & Howland, 1987, Schaeffel, Howland & Farkas, 1986, Vilupuru & Glasser,

2002). In each experiment, a calibration curve was generated to relate the slope of the vertical brightness profile through the pupil to the absolute refractive state of the eye obtained with the previous Hartinger coincidence refractometer measurements. The dynamic photorefractive optical change occurring in the eye during centrally stimulated accommodation was recorded onto videotape, and subsequent image analysis was performed to measure the pupil brightness profile. The calibration curve was then used to relate the dynamic changes in the pupil brightness profile to the accommodative amplitude.

2.4 Dynamic biometric measurements

Biometric changes were measured with continuous high-resolution A-scan ultrasound biometry (CUB) (Beers & van der Heijde, 1994, Vilupuru & Glasser, 2005). Biometric measurements were recorded to a computer at 100 Hz, using a 10-MHz transducer. The transducer contacted the cornea through ultrasound transmission gel to generate sharp A-scan peaks representing the anterior and posterior cornea surfaces, anterior and posterior lens surfaces, and the retina. The CUB measures the time between peaks associated with the intraocular surfaces. These times are converted to distances using standard, accepted sound velocities: anterior and vitreous chambers, 1532 m/s and lens, 1641 m/s (van der Heijde & Weber, 1989, Vilupuru & Glasser, 2005). Biometric changes were recorded during a sequence of increasing EW-stimulated accommodative responses. The same stimulus current amplitudes used during the photorefraction described earlier were used for the CUB measurements.

2.5 Dynamic measurement of phakometry and lens tilt and decentration

A custom-built dynamic (30 Hz) video-based phakometer was used to measure lens radii of curvature and lens tilt and decentration. The set-up included a broad spectrum, white light source, two collimated optic fibers (to assure that the Purkinje images are in focus) and a video camera with a telecentric lens to capture the reflections produced by the anterior cornea (PI), and the anterior and posterior lens surfaces (PIII, PIV). This system was modified from that described previously in the literature (Mutti, Zadnik & Adams, 1992). The collimated light sources used for illumination were adjustable and were separated horizontally between 5-10 deg from the optical axis of the camera for

the measurements. Both phakometry and lens tilt and decentration data were calculated from the same measurements using the double light sources. Measurements were performed with a plano perfusion speculum lens filled with saline solution placed over the monkey's cornea to effectively neutralize the cornea and improve Purkinje image visibility. This was a custom made lens with an open circular base designed to fit under the eye lids against the conjunctiva concentrically around the limbus. The lens held a 5 ml volume chamber in front of the cornea with a plano clear glass cover slip on the front with an inlet and an outlet tube to fill the chamber in front of the cornea with normal buffered saline. To calculate anterior and posterior lens radii of curvature, the heights of PIII and PIV relative to PI (h3/h1 and h4/h1 respectively), were measured frame-by-frame from the recorded video phakometry images. Corneal curvature, measured from a linear calibration curve obtained from calibrating the phakometer on a set of steel calibration ball bearings of different, known radii, and lens thickness and anterior chamber depth measured with A-scan ultrasound biometry, were used in the calculations, using the equivalent mirror theorem (Smith & Garner, 1996) and an iterative method (Garner, 1997) with custom routines written in Matlab (Rosales & Marcos, 2006).

To measure lens tilt and decentration a linear relationship between Purkinje image locations, eye rotation β, lens tilt α and lens decentration d was assumed according to Phillips' linear equations (Phillips, Perez-Emmanuelli, Rosskothen & Koester, 1988).

$P1 = E\beta;\ P3 = F\beta + C\alpha + Ed;\ P4 = G\beta + D\alpha + Fd$; $P1$, $P3$ and $P4$ are the relative locations of the midpoint of the double PI, PIII and PIV Purkinje images and A, B, C, D, E, F and G are coefficients that depend on the individual ocular biometry, (see Chapter 2 for details). Since the eyes were iridectomized, the pupil center could not be located and therefore be used as a reference for PI, PIII and PIV. Alternatively, we used the midpoint of the double PI as a reference. Considering that the head was not rotated, and head and eye rotation did not change with accommodation (the first Purkinje image did not move significantly with accommodation (less than 0.0001mm) this approximation should be appropriate. To calculate the coefficients of the Phillips equations, eyes were modeled using Zemax with measured A-scan biometric parameters and lens radii obtained from phakometry measurements following the procedures described in detail previously (Rosales & Marcos, 2006), Chapter 2.

To evaluate the validity of these algorithms on a monkey eye with the corneal neutralizing profusion lens in front of the eye, computer simulations were performed with the lens on the eye. A model eye was built in Zemax with anterior and posterior lens radii of 9.09 mm and -5.93 mm respectively. The Purkinje images for the monkey eye and the experimental configuration were simulated and the simulated images were processed with the same algorithms used for processing the real images. Anterior and posterior lens radii were calculated with an accuracy of 0.11 and 0.07 mm respectively. Similarly, an eye was simulated with nominal values for tilt and decentration of 1 deg and 5 deg for tilt around the vertical axis and tilt around the horizontal axis, and 0.5 mm and 0.1 mm for horizontal and vertical decentration. Tilt and decentration were calculated with an accuracy of 0.089 deg and 0.009 mm respectively with respect to the nominal values.

2.6 Experimental protocols

Monkeys were initially anesthetized with intramuscular ketamine (10 mg/kg) and acepromazine (0.5 mg/kg). Surgical depth anesthesia was induced with an initial bolus of 1.5 mg/kg followed by constant perfusion at 0.5 mg/kg/min of intravenous propofol (Propoflo, Abbott Laboratories, North Chicago, IL).

The anesthetized monkeys were placed prone with the head held in a head holder, upright and facing forward for all measurements. At the beginning of each experimental session, sutures were tied beneath the medial and lateral rectus muscles of the monkey eye and light tension applied by micrometers to reduce convergent eye movements. The eyelids were held open with lid speculums. A plano polymethyl-methacrylate contact lens was placed on the cornea for refraction measurements to maintain optical quality and prevent dehydration. Five, four-second duration stimulus trains (600-μs pulse duration, 72 Hz, amplitude range 10 to 2,000 μA) with a four-second inter stimulus interval were used to induce varying amplitudes of accommodation. The accommodative response to three different current amplitudes was first measured using a Hartinger coincidence refractometer. The same increasing stimulus amplitudes were used for the same monkey throughout the session. Infrared video photorefraction was performed with a contact lens on the cornea. Video phakometry was then performed, with the corneal neutralizing perfusion speculum. Finally, because it was a contact procedure, A-scan ultrasound biometry was performed with ultrasound transmission gel

on the cornea. For monkey #54, one eye was measured per session over approximately 2 hours, one month apart. For monkey #58 both eyes were measured in the same session. For each procedure and for each stimulus amplitude, only the last three of the five stimulus trains were analyzed.

Lens tilt and decentration were calculated for the un-accommodated state and accommodative responses for the different current stimuli. Because the tilt and decentration calculations were more computationally demanding, this analysis was not done on all dynamic data traces. Instead, a total of 15 images were analyzed from the last three stimuli. Six images were captured when the stimulus was OFF and 9 images were captured when the stimulus was ON near the end of the stimulus train when the eye was in a stable and maximally accommodated state for each of three different increasing stimulus amplitudes. The images were captured during each of the last three stimuli. The corresponding averaged optical biometry data, for the corresponding stimulation sequences were used for data processing.

3. RESULTS

3.1 EW stimulated accommodation

Figure 6.1 shows the Hartinger measured accommodative response for each stimulus current amplitude for the four eyes. These functions were used to convert the stimulus current amplitudes into actual accommodative response for the photorefraction calibration procedures.

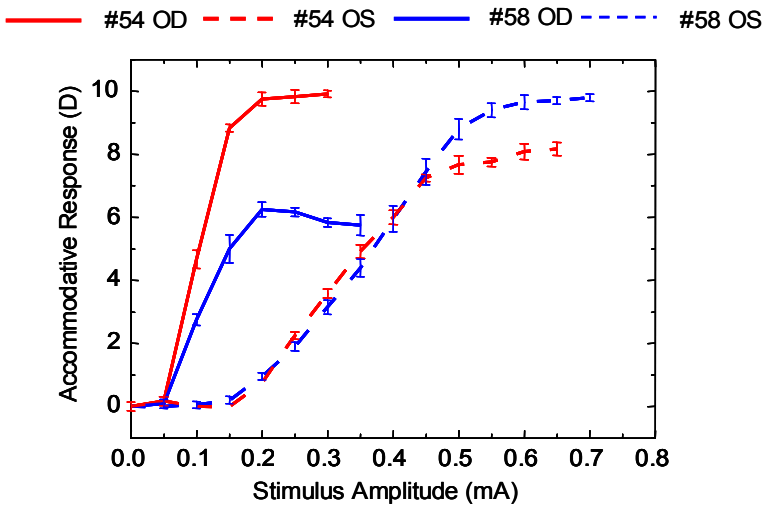

Figure 6.1. Accommodative response for each current stimulus for the four eyes of the two monkeys used in this experiment. Each point is the average of three measurements. Error bars are standard deviations.

Maximum accommodative response amplitudes were 9.91 D for monkey #54 OD, 7.75 for monkey #54 OS, 5.75 D for monkey #58 OD and 9.65 for monkey #58 OS.

In this experiment, the accommodative response for a given current stimulus varied across eyes, and between eyes of the same monkey, dependent on the anatomical position of the stimulating electrode.

3.2 Dynamic photorefraction and biometry

Photorefraction, anterior chamber depth and lens thickness, were recorded dynamically at 30 Hz. These measurements, along with the dynamic recording of the Purkinje images, allowed dynamic changes in lens curvatures to be calculated. Figure 6.2 shows an example of dynamic recoding of photorefraction, and optical biometry for monkey #54 OS, for one stimulus (off-on-off). The abrupt step trace at the bottom of the graph indicates the start, duration (four seconds) and termination of the stimulus train. Anterior chamber depth (ACD) decreases systematically and lens thickness (LT) increases systematically with accommodation. These dynamic data recorded at 30Hz were used, along with 30 Hz phakometry images, for calculations of lens radii of curvature and lens tilt and decentration for the same accommodative levels. The repeatability of EW stimulated accommodative responses has been demonstrated in previous studies (Glasser et al., 2006, Vilupuru & Glasser, 2005), temporal registration of the different measurements is possible to within 1/30 of a second (i.e., at the video frame rate).

Figure 6.3 shows dynamic biometric changes (anterior chamber depth and lens thickness) with accommodation for all eyes. Data are from the last stimulus producing the maximum accommodative amplitude.

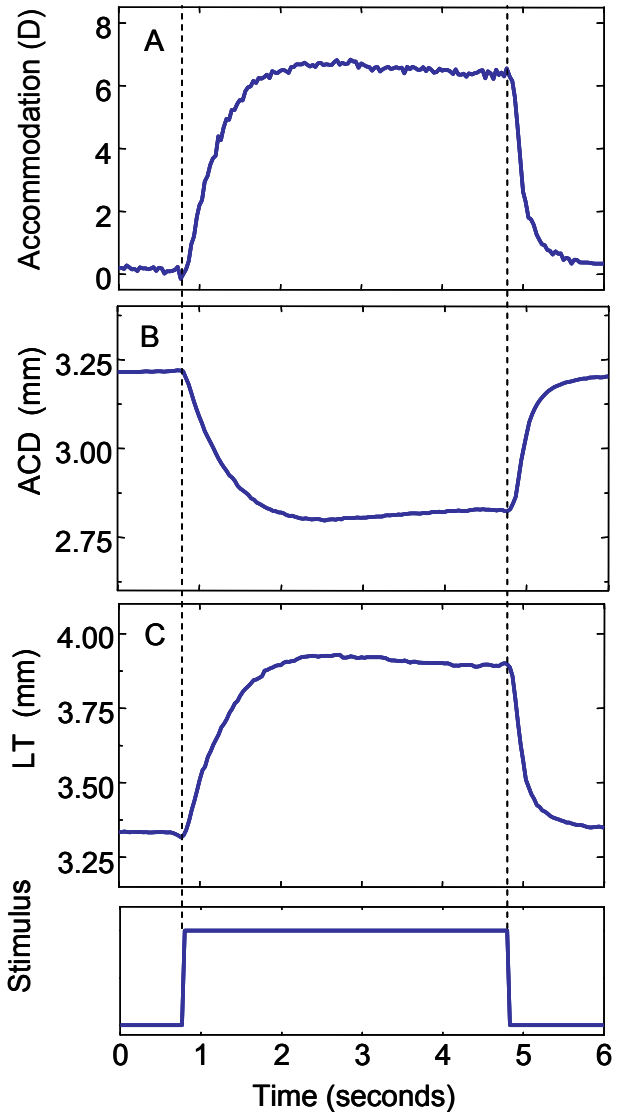

Figure 6.2. Dynamic recordings of accommodation from photorefraction and lens thickness (LT) and anterior chamber depth (ACD) from continuous ultrasound biometry (CUB) from monkey #54 OS, for an accommodation response of 7.75D. Photorefraction was measured first, followed by the CUB measurements for the same stimulus amplitude. This example corresponds to a single response (the 5th response to five, four-second long stimuli).

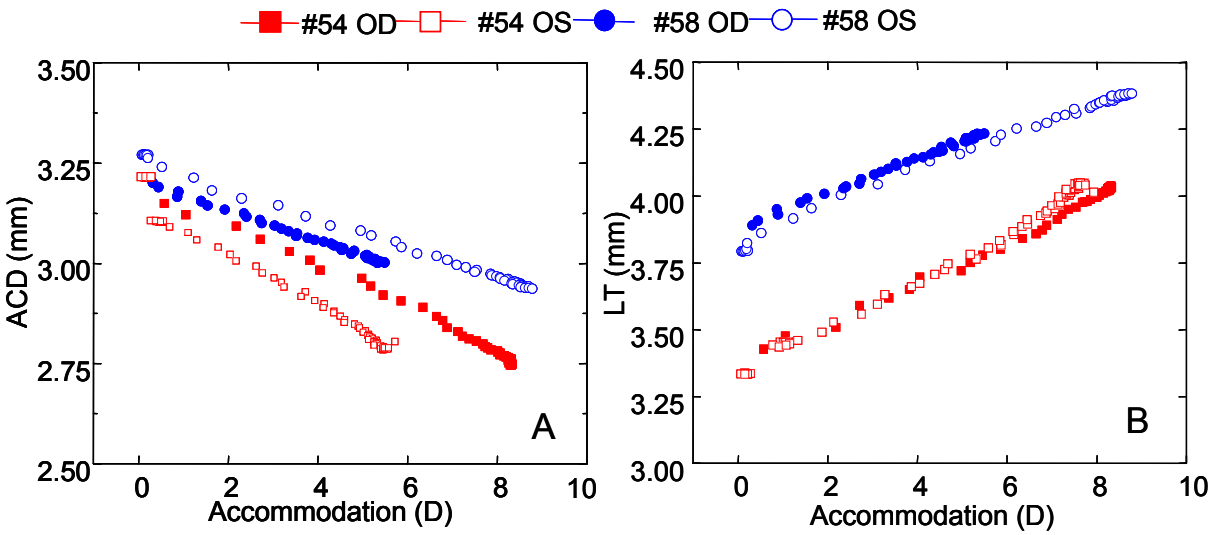

Figure 6.3. Dynamic biometric changes (anterior chamber depth and lens thickness) with accommodation for all eyes. Data are from the last stimulus producing the maximum response with accommodation recorded first with photorefraction and ACD and LT recorded subsequently with the CUB.

Figure 6.4 shows an example of changes in anterior and posterior lens radii of curvature for monkey #54 OS for the same stimulus sequence as shown in Figure 6.2.

Average unaccommodated anterior and posterior lens radii were 11.11±1.58 mm and -6.64±0.62 mm respectively and decrease (in absolute values) systematically with accommodation in all eyes (Figure 6.5). Average values were obtained from the last three of the five stimuli applied. For the same accommodative level there are individual differences in the anterior and posterior radii of curvatures. The amounts and rate of change tend to be similar across eyes of the same monkey.

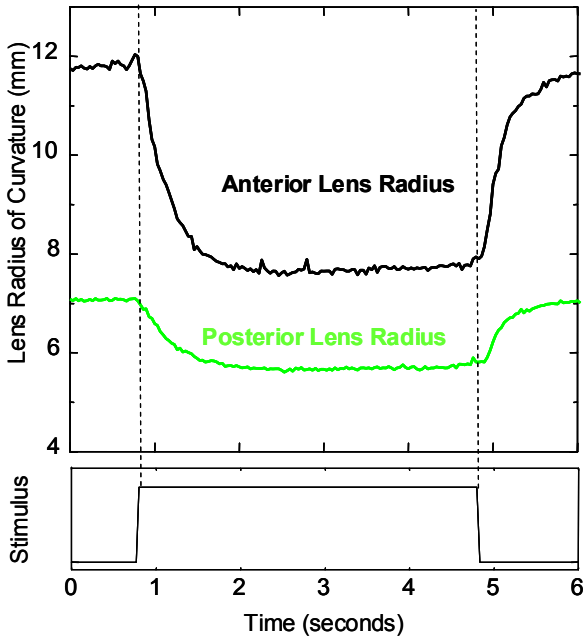

Figure 6.4. Anterior and posterior lens radii of curvature as a function of accommodation, for a phakometry sequence (5th stimulus). Phakometry data were calculated using individual biometry data shown in Figure 2, for monkey #54 OS.

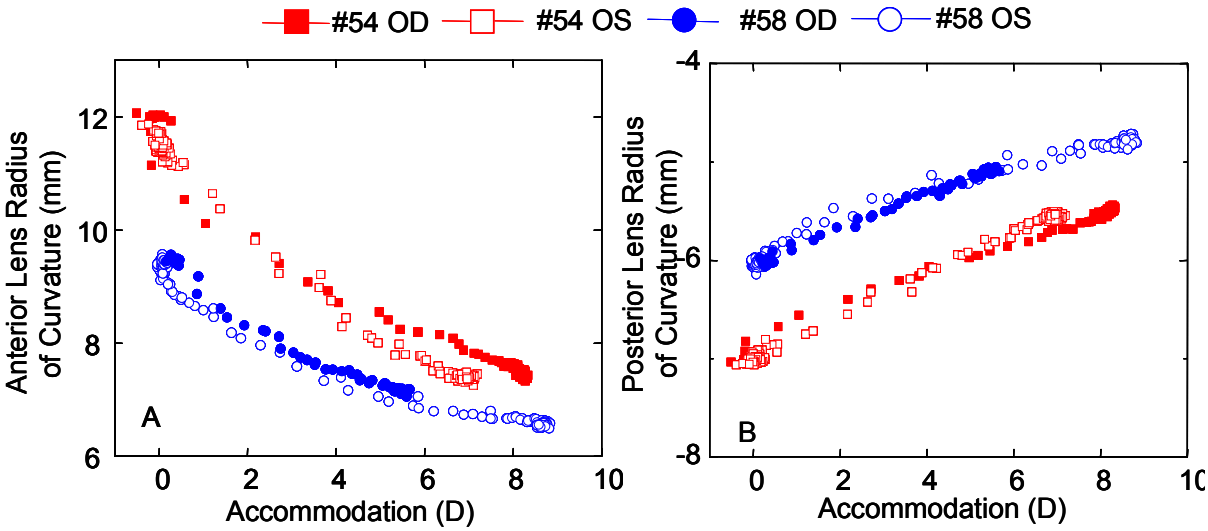

Figure 6. 5. Anterior and posterior lens radii of curvature as a function of accommodation for both eyes each of monkey #54 and monkey #58. Data are from the 5th stimulus for the maximum accommodative response in the phakometry sequence. Biometry and photorefraction data from each individual eye, corresponding to that shown in Figure 2, were used in the data processing.

A better comparison of the rate of decrease in radii of curvature across eyes can be performed by relating all values to the unaccommodated state. Figure 6.6 shows average changes in radii of curvature as a function of accommodation, relative to the unaccommodated state, averaged across eyes. Since the accommodative responses differed across eyes, spline fitting to the data was performed to average across the individual data from each eye. The curves in Figure 6.6 show similar slopes for the anterior and posterior surface (0.0058 mm^{-1}/D and 0.0056 mm^{-1}/D respectively, averaging across eyes and monkeys), indicating that both surfaces contribute similarly to change in power. The curves are relatively linear for the first 4 D indicating that the relative contribution of the surfaces to the lens power change is rather constant with accommodation.

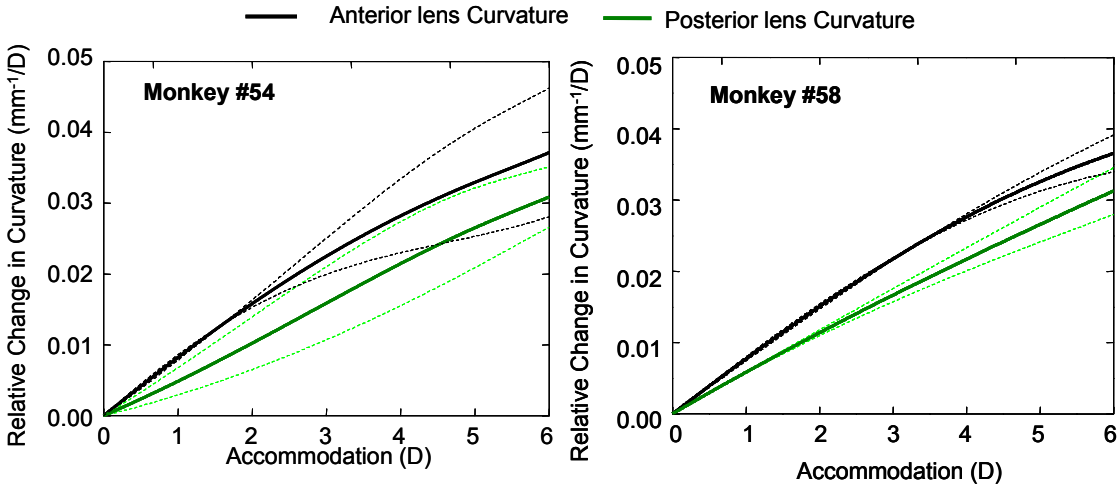

Figure 6.6. Average changes in anterior and posterior curvature relative to the un-accommodated state from the two monkeys. Data for each eye was fitted using a spline function, and then averaged across eyes for each monkey at different accommodation levels. Dashed lines represent ± 1 standard deviation.

3.3 Changes in lens tilt and decentration with accommodation

Table 6.1.a and Table 6.1.b show measurements of tilt and decentration (horizontal and vertical components) for each eye. See Chapter 2 (page 56, Figure 2.6) for sign conventions.

Table 6.1.a Lens tilt (α in degrees) and decentration (d in mm) for 0 D of accommodation for all eyes

	α_x	α_y	d_x	d_y
#54 OD	8.97±0.03	-1.09±0.03	0.17±0.01	1±0.01
#54 OS	8.08±0.04	-1.81±0.04	0.17±0.01	0.56±0
#58 OD	3.22±0.06	0.25±0.05	-0.05±0.01	0.95±0.01
#58 OS	2.48±0.05	-0.13±0.15	0.13±0.02	0.79±0.01

Table 6.1.b Lens tilt (α in degrees) and decentration (d in mm) for the maximum accommodation amplitude for all eyes

	α_x	α_y	d_x	d_y
#54 OD	9.63±0.11	-1.3±0.12	0.18±0.02	0.94±0.02
#54 OS	6.69±0.2	-0.99±0.12	0.04±0.01	0.44±0.02
#58 OD	5.08±0.15	0.73±0.12	-0.07±0.02	1.03±0.02
#58 OS	6.24±0.18	-1.03±0.13	0.11±0.02	0.92±0.01

Average unaccommodated lens tilt around the vertical axis was 5.69±3.31 deg and average tilt around the horizontal axis was -0.69±0.93 deg. Average unaccommodated lens decentration was 0.10 ± 0.11 mm horizontally and 0.82 ± 0.20 mm vertically. With accommodation, tilt around the horizontal axis increases significantly ($p<0.0044$) for all eyes except for #54 OD. The largest increase occurred for eye #58 OS, for which tilt around the horizontal axis increased at a rate of 0.39 deg/D (a total increase of 3.77 deg between 0 and 9.7 D of accommodation). Tilts around the vertical axis were much smaller than tilts around the horizontal axis. Decentration did not change significantly with accommodation in any of the eyes.

4. DISCUSSION

Dynamic accommodative measurements of the anterior and posterior lens radii of curvature and lens tilt and decentration have been presented for the first time in monkey eyes. These measurements are important to fully characterize the accommodative mechanism in Rhesus Monkey eyes. Comparisons of the ocular changes measured here during accommodation in monkeys with those measured in humans will further serve to test the extent of the similarity. This study was primarily directed at measuring lens radius of curvature, tilt and decentration, and how they change during accommodation. For the unaccommodated state, average anterior lens radius of curvature of 11.11±1.58

mm and posterior lens radius of curvature of -6.64±0.62 mm were found from the four eyes of the two monkeys. These values are close to the values reported for a four-surface schematic eye of macaque monkey obtained by an optical method (Lapuerta & Schein, 1995). Results obtained here for the anterior and posterior lens radii in monkeys using a collimated light source were not significantly different between the equivalent mirror theorem and the merit function. In previous studies (Rosales, Dubbelman, Marcos & Van der Heijde, 2006, Rosales & Marcos, 2006) a difference between the two algorithms was found, very likely due to the use of an uncollimated light source. Accommodative changes in monkeys of -0.48±0.14 mm/D and 0.17±0.03 mm/D for the anterior and posterior lens radii of curvature were found using a Purkinje imaging method in the present study. In terms of changes of curvature per diopter of accommodation, those slopes would be 0.006 mm^{-1}/D and 0.00485 mm^{-1}/D for the anterior and posterior lens respectively. A prior study using drug stimulated accommodation in monkey eyes found approximately -0.272 mm/D and 0.215 mm/D for the anterior and posterior lens using Scheimpflug imaging in two eyes of one monkey (Koretz, Bertasso, Neider, True-Galbelt & Kaufman, 1987b).

Changes in lens radii of curvature with accommodation in human eyes differ across studies. Some studies found changes in the human eye which are close to the results of the present study in monkey eyes. For example, Koretz (Koretz, Cook & Kaufman, 2002), using Scheimpflug on one 19 year old human subject found a mean change of -0.33 mm/D and 0.15 mm/D, for the anterior and posterior lens radii of curvature, respectively.

However, while most studies report similar changes for the posterior lens, in general larger changes are measured for the anterior lens in humans than those found in the present study for monkeys. Garner (Garner & Yap, 1997) using Purkinje imaging found a value of -0.62 mm/D and 0.17 mm/D for anterior and posterior lens radii on average in a group of 11 young eyes (21.2±2.6 years). Dubbelman (Dubbelman, van der Heijde & Weeber, 2005), also using Scheimpflug imaging, found changes of -0.62 mm/D and 0.13 mm/D for the anterior and posterior lens radius of curvature respectively (0.0067 mm^{-1}/D and 0.0037 mm^{-1}/D in terms of curvature).

Differences across studies are not necessarily associated with the technique (Scheimpflug or Purkinje imaging). In a recent study, similar values for anterior and posterior lens radii of curvature with accommodative effort were found using Scheimpflug (-0.64±0.04 and 0.23±0.08 mm/D for the anterior and posterior lens

radius of curvature respectively) or Purkinje imaging (-0.57±0.05 and 0.29±0.04 mm/D for the anterior and posterior lens radius of curvature) on the same human eyes (mean age: 28.5) (Rosales et al., 2006).

The fact that most previous human studies relate phakometry measurements to accommodative demand rather than to the actual accommodative response, cannot be the cause for the discrepancy, since compensation for the accommodative lag would increase the relative mm/D accommodative changes of the radii of curvature, rather than decrease them. Although a direct comparison between results obtained from monkey and human eyes can not be done, due to differences in eye size and different experimental protocols (contralateral accommodation; pharmacological, natural or centrally stimulated accommodation or differences in the ages of the subjects) the results presented here suggest that change in anterior radius of curvature per diopter of accommodation is lower in iridectomized monkeys than in human eyes, indicating than other factors (i.e. gradient index distribution or lens surface asphericity) may play a role in the change of lens power with accommodation.

When the unaccommodated radii of curvature and the accommodative change in lens curvatures for 10 D of accommodation found in the present study are applied to a monkey schematic eye (Lapuerta & Schein, 1995) using the Bennett-Rabbets schematic eye model (Bennett & Rabbetts, 1984), with a uniform equivalent refractive index lens, this accounts for only 7.8 D of accommodation. If a gradient refractive index (GRIN) model was used, the reported differences in lens radii of curvature between monkeys and humans would be even larger and would result in a relatively larger contribution of GRIN to the crystalline lens power change with accommodation in monkeys than in humans.

Some authors have attributed a role of the iris in modifing the shape of the anterior lens with increased accommodation (McWhae & Reimer, 2000). However, the absence of iris in the monkeys in this study cannot be the cause of any differences between humans and monkeys. It has been shown that removal of the iris does not affect the EW stimulated accommodative amplitude in monkeys (Crawford, Kaufman & Bito, 1990). Further, in the present study the optical accommodative response, as well as the accommodative biometric changes were actually measured, so the calculated changes in curvature were related to the actual accommodative change in refraction, lens thickness and anterior chamber depth that occurred.

A factor that may produce an underestimation of lens radii of curvature is the fact that primate lenses are in fact aspherical surfaces. The influence of asphericity on the Purkinje estimates of lens radii was analyzed in depth in a previous study (Rosales & Marcos, 2006). This study found that, particularly for the anterior surface, asphericity had a minimal influence on the lens radius of curvature estimates. However, in the previous study the lens area was limited by the pupil, and therefore probably closer to the apical region. In the iridectomized monkey eyes, where no constraints are imposed by the iris, the Purkinje images were reflected off more peripheral regions of the lens where the asphericity may be a more important factor.

The values obtained for tilt and decentration in this study on monkeys are larger than those found in prior studies in humans (Chapter 2). Part of the differences may be due to a systematic accommodative decentration of the pupil center (used as a reference in the previous study) with respect to the midpoint of the first double Purkinje image (used as a reference in the present study, due to the absence of the pupil in the iridectomized eye). Pupil decentration affects both the reference for decentration, as well as the reference axis for tilt (which was the pupillary axis in previous studies). In the monkey experiments the eye did not converge during accommodation**.** Therefore, while the absolute values of tilt and decentration are likely affected by the choice of reference axis, the relative changes of lens tilt and decentration with accommodation are not. The relative changes of decentration and tilt with accommodation were systematic except for one monkey eye and higher for tilt around the horizontal axis than tilt around the vertical axis and decentration. To our knowledge the only report of lens tilt and decentration in human eyes for unaccommodated versus accommodated states was unable to find statistical differences (Kirschkamp et al., 2004). Data in that study were only for the horizontal meridian, for an accommodative demand of 4D.

Lens tilt and decentration can have an effect on ocular aberrations. In Chapter 8 (Rosales & Marcos, 2007) we will study the effect of real amounts of tilt and decentration in human eyes with intraocular lenses. In normal human eyes, asymmetric aberrations (such as coma) do not change systematically with accommodation (He et al., 2000), although one study reports minor changes of coma in some subjects, particularly in the vertical direction (Plainis et al., 2005). Also, previous observations in monkeys during centrally stimulated accommodation are consistent with significant changes in lens tilt and decentration, particularly in the vertical direction (Glasser & Kaufman, 1999). The greater tilt of the lens around the horizontal axis reported in the present

study is consistent with the observation that gravity influences the movement of the crystalline lens during accommodation in monkeys (Glasser & Kaufman, 1999). Also the change in tilt with accommodation may affect high order aberrations, particularly coma. Vertical coma has been shown to increase significantly and systematically with increasing accommodation compared to the unaccommodated state in some centrally stimulated iridectomized monkey eyes (Vilupuru et al., 2004). Changes in horizontal coma were not significant (Glasser personal communication), which is supported by the small amounts of tilt around the vertical axis and horizontal decentration found in the present study. Customized computer eye modelling shows that lens tilt tends to compensate the optical effects produced by eye rotation (Rosales & Marcos, 2007). It is certainly possible that the tension induced with sutures to minimize accommodative convergent eye movements as used in this study, may impact the tilt and decentration results reported here. Also, the systematic changes in tilt that appear to occur with EW stimulated accommodation in at least some anesthetized rhesus monkeys may stem from several factors. EW stimulation may produce greater contractions of the ciliary muscle than could occur with voluntary accommodation. The rhesus monkey ciliary muscle may be capable of far greater accommodative excursions than the human ciliary muscle. EW stimulated accommodation in young rhesus monkeys can produce 15 D or more of accommodation, whereas 10 D is nearing the upper limit of voluntary accommodation in young humans. Further, the presence of the iris, especially when constricted during accommodation, may provide greater stability to the lens than in iridectomized eyes.

In conclusion, dynamic phakometry, tilt and decentration were measured for the first time in monkey eyes during accommodation using Purkinje imaging. Changes in the lens radii of curvature with accommodation are consistent with those found in human eyes, with the anterior lens getting steeper at a faster rate. Tilt, particularly around the horizontal axis, changed significantly with accommodation in some eyes, apparently more than in human eyes. No significant changes in lens decentration were found. These results are important to fully characterize the accommodation mechanism in monkey eyes, to understand the age changes that occur in the accommodative mechanism, as well as for the evaluation and design of strategies for presbyopia correction, for example lens refilling (for which the relative contribution of lens curvature and refractive index is critical).